

Temperature difference between the body core and arterial blood supplied to the brain during hyperthermia or hypothermia in humans

Maitreyi Bommadevara, Liang Zhu

Abstract A vascular heat transfer model is developed to simulate temperature decay along the carotid arteries in humans, and thus, to evaluate temperature differences between the body core and arterial blood supplied to the brain. Included are several factors, including the local blood perfusion rate, blood vessel bifurcation in the neck, and blood vessel pairs on both sides of the neck. The potential for cooling blood in the carotid artery by countercurrent heat exchange with the jugular veins and by radial heat conduction to the neck surface was estimated. Cooling along the common and internal carotid arteries was calculated to be up to 0.87 °C during hyperthermia by high environmental temperatures or muscular exercise. This model was also used to evaluate the feasibility of lowering the brain temperature effectively by placing ice pads on the neck and head surface or by wearing cooling garments during hypothermia treatment for brain injury or other medical conditions. It was found that a 1.1 °C temperature drop along the carotid arteries is possible when the neck surface is cooled to 0 °C. Thus, the body core temperature may not be a good indication of the brain temperature during hyperthermia or hypothermia.

1

Introduction

Monitoring the temperature of the brain has many applications in physiology and medicine. Generally, the temperature of the human brain is not measured directly because of concern for inducing damage by the introduction of temperature probes. Clinically, it is usually assumed that brain temperature is equal to the core body temperature. However, during hyperthermia or hypothermia, the core body and brain temperatures may be quite different. In this study a theoretical approach is developed to simulate the temperature difference between the brain and body core and to evaluate the effect of various factors on this temperature difference.

Theoretical and experimental studies suggest that there should exist a small temperature variation in the human brain under normothermic conditions because of its high blood perfusion rate. The temperature of the brain is typically close to that of the internal carotid arterial blood before the blood enters the Circle of Willis (Zhu and Diao 2001). Under normothermic conditions, it has been shown that the temperature along the common and internal carotid arteries does not change significantly due to the relatively small heat exchange surface of the blood vessels and high flow velocity of the blood. However, when the surfaces of the neck and head are cold due to either sweating or wearing external cooling garments, heat loss from the common and internal carotid arteries may result in a 1 to 2 °C temperature drop in the carotid arterial blood before it enters the Circle of Willis (Zhu 2000). Thus, under those circumstances, the core body temperature is no longer a good indication of the brain temperature.

The normal core temperature of a healthy resting adult human being is around 37 °C. During hyperthermia caused by a high environmental temperature or muscular exercise, the core temperature may rise to as high as 42 °C without permanent ill effects (Cabanac 1993). It is well known that brain tissue has a lower thermal tolerance than the rest of the body. Selective cooling of the warm arterial

Received: 10 January 2002 / Accepted: 7 May 2002

M. Bommadevara, L. Zhu (✉)
Department of Mechanical Engineering,
University of Maryland Baltimore County,
Baltimore, MD 21250, USA
e-mail: zliang@umbc.edu
Fax: +1-410-4551052

This research was supported by a UMBC Summer Faculty Fellowship.

blood before it reaches the base of the brain has been suggested as the natural reaction of the body to mitigate overheating of the extremely heat-susceptible cerebral tissue (Cabanac 1993; Zhu 2000). Whether this mechanism, which has been demonstrated in some animals (Baker 1982), also operates in humans is still controversial. The points of contention are the potential for cooling blood in the carotid artery and the interpretation of the experimental and theoretical results. Nielsen (1988) observed that the measured tympanic temperature was significantly lower than the core body temperature during cold outdoor exercise. Several researchers (Cabanac 1993; Zhu 2000) have suggested that blood is cooled in the arteries by countercurrent heat exchange between the carotid artery and the jugular vein, where the venous blood could be significantly cooled by evaporation at the head and facial surfaces. Zhu (2000) calculated the relative contributions to selective brain cooling of countercurrent heat exchange and radial heat conduction to the neck surface, and found that the two mechanisms are comparable. During normal or hyperthermic conditions, the neck and head surfaces may be cold due to cold air temperature, high wind speed, low humidity, or intensive sweating on the skin surface.

Several medical applications involve head and neck cooling garments. Cold fluid flows through internal channels of these garments, and cold surfaces of the neck and head can be achieved if good thermal contact between the internal surface of the garment and the skin is maintained. It is well known that heat has an adverse effect on the neuromotor performance of humans. Hyperthermia usually degrades the neurological outcome in patients suffering neurological disorders or head injury. In multiple sclerosis patients, the symptoms are typically exacerbated with elevated body temperature. Clinical study has suggested that wearing a head and neck cooling garment could alleviate symptoms of multiple sclerosis and prevent increased core temperature during daily activities (Ku et al. 1996). Ku et al. also found that head and neck cooling reduced the core temperature of both men and women to the extent required for symptom management of certain neurological patients. It is not clear from their study whether the symptomatic relief in multiple sclerosis patients was related to the possible temperature decrease in the body core and/or in the arterial blood supplied to the brain.

In recent years, mild or moderate hypothermia has been proposed for clinical use as an adjuvant for achieving protection from cerebral ischemia and traumatic brain injury (Barone et al. 1997; Marion et al. 1997; Sirimanne et al. 1996). Experimental studies have demonstrated that mild or moderate hypothermia reduces mortality compared to normothermia or hyperthermia in rats after controlled severe cortical impact (Clark et al. 1996). It has been shown that a reduction in brain temperature as small as 2 °C reduces ischemic cell damage (Clark et al. 1996) or significantly improves post-ischemic regional histopathology (Wass et al. 1995), in contrast to fever-induced hyperthermia (>1°), which worsens the neurological outcome in a canine model of complete cerebral ischemia (Wass et al. 1995).

Clinically feasible brain cooling methods include a head hood or helmet with chemical or water cooling, head immersion in ice water, and nasopharyngeal cooling after tracheal intubations. Among them, wearing a cooling helmet is noninvasive and easy to implement. The temperature of the cooling fluid inside the helmet may be as low as 0 °C. Under those circumstances, radial heat conduction from the warm arterial blood to the cold neck surface may be greatly enhanced to achieve a reduction in brain temperature.

Several theoretical studies calculated the temperature decrease along the carotid artery before it reaches the base of the brain. Based on previous theoretical studies (Nielson 1988; Nunneley and Nelson 1994; Wenger 1987; Wu et al. 1993), Zhu (2000) developed a theoretical model to simulate the temperature distribution along the carotid artery in the neck. This appears to be the most comprehensive theoretical model developed to describe the blood-tissue thermal interaction in the neck. However, there are several limitations associated with this model: (i) the tissue was modeled as a purely conductive media with one pair of large blood vessels, and the convective effect of the smaller blood vessels in the tissue was not considered; (ii) no blood vessel bifurcation was taken into consideration; and (iii) thermal interaction between blood vessel pairs on both sides of the neck was neglected. A mixed model, accounting for the contributions of different sized blood vessels, is necessary to describe the blood-tissue thermal interaction in the neck based on a more realistic vascular anatomy in the neck.

In this research, a theoretical model is developed to study thermal equilibration in the countercurrent vessel pairs in the human neck based on the analyses in Zhu (2000) and Weinbaum et al. (1997). In this approach, large blood vessels such as the common, internal, and external carotid arteries, and the internal and external jugular veins are modeled individually on both sides of the tissue cylinder of the neck, while the smaller blood vessels bifurcating from the large blood vessels are modeled by a modified blood perfusion term. The temperature distribution along the carotid arteries

is then calculated for both hyperthermic and hypothermic conditions. Various factors that may affect this temperature distribution are evaluated and discussed.

2

Mathematical formulation

Heat exchange between the countercurrent blood vessel pairs and the surrounding tissue in the neck can be described by the schematic diagram shown in Fig. 1, in which an axially uniform tissue cross section is assumed. The internal and external jugular veins are modeled as two straight tubes located symmetrically on each side of the neck. The common carotid artery present on either side of the neck bifurcates into internal and external carotid arteries. It is assumed that the internal and external carotid arteries run obliquely toward the center and the skin surface of the neck, respectively. Based on the anatomical consideration, the neck tissue is divided into two regions, as shown in Fig. 1. There is no axial variation in the vessel and the tissue cross-sectional planes in region 1, while in region 2, both vessel eccentricity s^* and vessel center-to-center spacing l^* vary in the axial direction.

Referring to Fig. 1, the principal assumptions of the model are as follows. Previous analysis suggests that the effect of unequal vessel size is small and produces less than 5% variation in the temperature decay (Weinbaum et al. 1997). Thus, to simplify the analysis in the cross-sectional plane, the artery and vein are assumed to be of the same diameter. For simplicity, the blood vessels are located symmetrically about the central axis of the neck cylinder, as shown in Fig. 1. The thermal properties for the blood and the tissue are assumed to be the same and homogenous within the neck (Chato 1985). A steady-state temperature field is assumed in the tissue and the vessels of the neck region. The velocity profile in the blood vessels is considered as parabolic. In this study the temperature at the neck surface is approximated as uniform. In the real situation, a small temperature variation at the neck surface is expected in the axial direction, while the neck surface temperature may vary significantly with the angle. Thus, the uniform neck surface temperature can be viewed as an average value of the temperature at the neck surface. Axial conduction in the neck tissue is neglected as previously justified (Zhu 2000). Axial conduction in the blood vessel is also neglected. This is a reasonable approximation since the Peclet number for blood flow in the vessels is greater than 2000, indicating that axial convection is the dominant mode for axial thermal equilibration in comparison with axial conduction. The temperature gradient $\partial T_{a,v}^*/\partial z^*$ in the convective term of the vessel governing equation is approximated by the axial gradient of the vessel bulk temperature $dT_{ab,vb}^*/dz^*$, as previously justified in Zhu et al. (1990). Finally, in this model the thermal effect of the small blood vessels in the neck region is modeled as a lumped heat source term as described by Weinbaum et al. (1997).

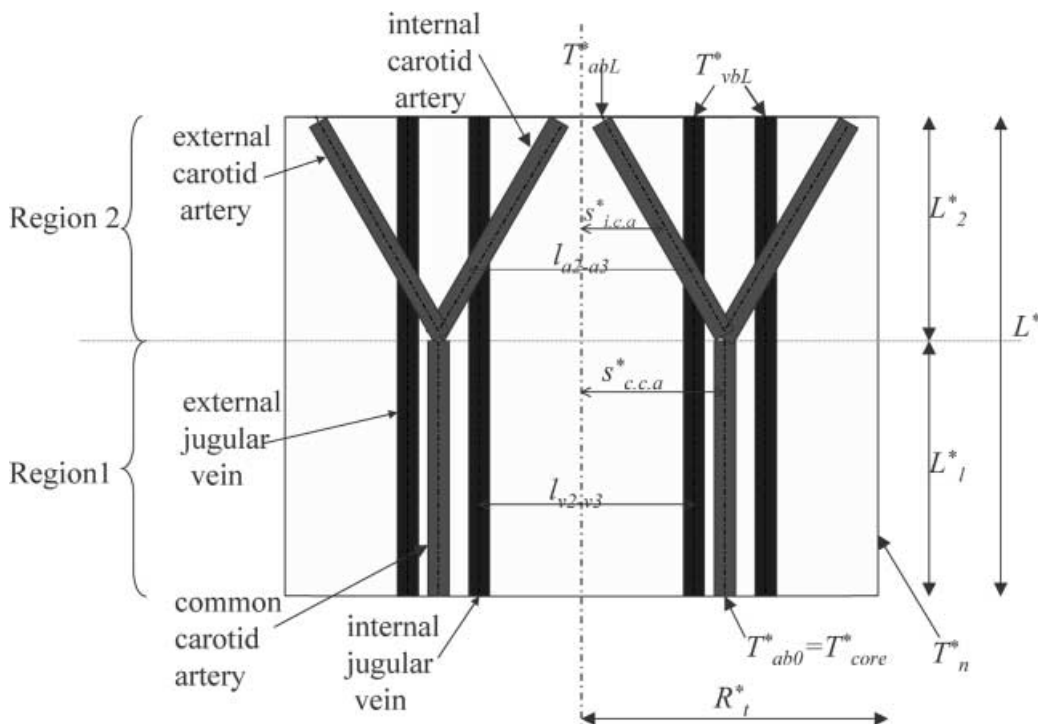


Fig. 1. Schematic diagram of the neck region with detailed vascular geometry

Figure 2 gives the cross-sectional plane of the neck tissue cylinder in region 1 and the cylindrical coordinate systems. Assuming homogeneous thermal properties within the tissue and blood in addition to the assumptions above, one could write the energy conservation equations for the artery, vein, and the tissue as follows:

$$k_{bl} \left\{ \left[\frac{1}{r_{ai}^*} \frac{\partial}{\partial r_{ai}^*} \left(r_{ai}^* \frac{\partial T_{ai}^*}{\partial r_{ai}^*} \right) \right] + \frac{1}{r_{ai}^{*2}} \frac{\partial^2 T_{ai}^*}{\partial \phi_{ai}^{*2}} \right\} = \rho_{bl} C_{bl} 2u_{ai}^* \left(1 - \frac{r_{ai}^{*2}}{a_{ai}^{*2}} \right) \frac{dT_{abi}^*}{dz^*}, \quad (1)$$

$$r_a^* \leq a_{ai}^*, \quad 0 \leq z^* \leq L, \quad i = 1, 2, 3, 4;$$

vein:

$$k_{bl} \left\{ \left[\frac{1}{r_{vi}^*} \frac{\partial}{\partial r_{vi}^*} \left(r_{vi}^* \frac{\partial T_{vi}^*}{\partial r_{vi}^*} \right) \right] + \frac{1}{r_{vi}^{*2}} \frac{\partial^2 T_{vi}^*}{\partial \phi_{vi}^{*2}} \right\} = -\rho_{bl} C_{bl} 2u_{vi}^* \left(1 - \frac{r_{vi}^{*2}}{a_{vi}^{*2}} \right) \frac{dT_{vbi}^*}{dz^*}, \quad (2)$$

$$r_{vi}^* \leq a_{vi}^*, \quad 0 \leq z^* \leq L, \quad i = 1, 2, 3, 4;$$

tissue:

$$k_t \left\{ \left[\frac{1}{R^*} \frac{\partial}{\partial R^*} \left(R^* \frac{\partial T_t^*}{\partial R^*} \right) \right] + \frac{1}{R^{*2}} \frac{\partial^2 T_t^*}{\partial \phi^2} \right\} = -0.7\omega \rho_{bl} C_{bl} [T_{abi}^*(z) - T_{t,avg}(z)], \quad (3)$$

$$R^* \leq R_t^*, \quad r_{ai}^* \geq a_{ai}^*, \quad r_{vi}^* \geq a_{vi}^*, \quad L^* \geq z^* \geq 0;$$

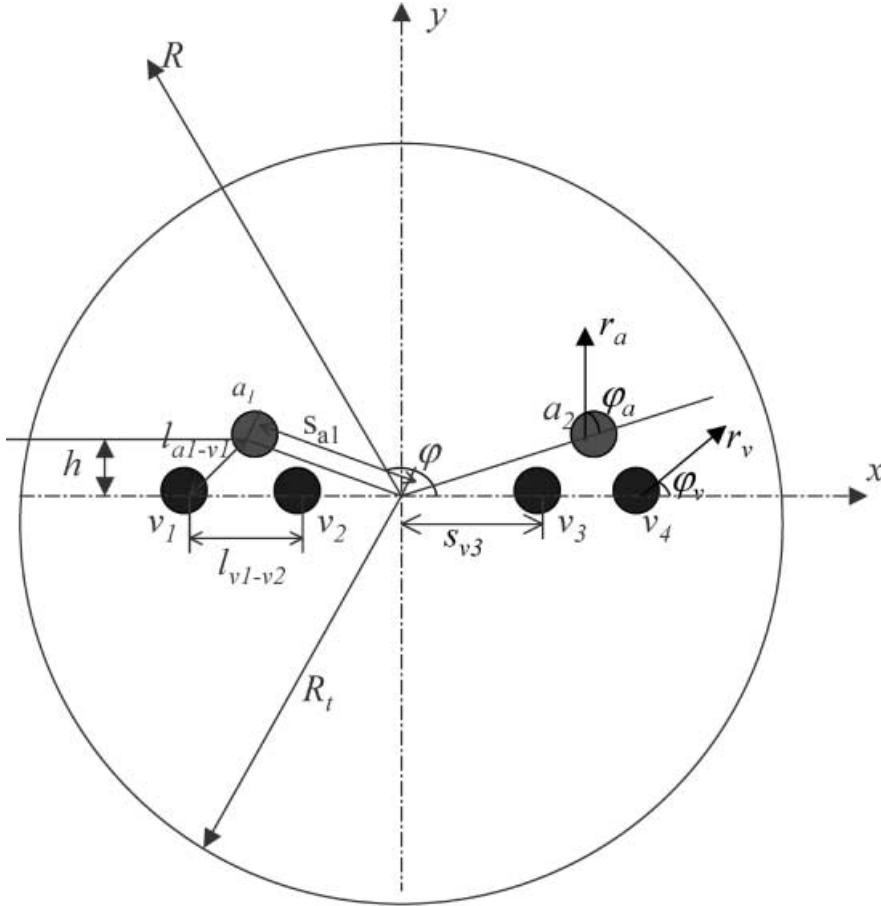


Fig. 2. Schematic diagram of the cross-sectional plane and the cylindrical coordinate system of region 1 in the model

(see Nomenclature). Note that the subscript i denotes the prescribed number of the artery or vein, and subscripts a, v, and t refer to artery, vein, and tissue, respectively. As shown in Fig. 3, there are two and four arteries in the cross-sectional plane in region 1 and region 2, respectively, while there are four veins in each region. The negative sign in the convective term in Eq. (2) is used to describe the opposite flow direction in the veins as compared with the arteries. On the right side of Eq. (3), ω is the local blood perfusion rate in the neck, and the coefficient 0.7 in the modified Pennes perfusion source term is an average value of the correction coefficient calculated by Weinbaum et al. (1997) for various muscle tissues. The quantity T_{abi}^* in Eq. (3) is the bulk temperature in either the common or the internal carotid artery and is defined below. In the modified perfusion source term in Eq. (3), $T_t^*(R, \phi, z)$ has been replaced by $T_{t,avg}^*(z)$, which is the average temperature of the tissue in the cross-sectional plane at the axial location z^* . Note that the maximum temperature variation in the cross-sectional plane is $T_{abi}^*(z) - T_n^*$. In general, the average temperature of the tissue has a value between the bulk temperature in the carotid artery $T_{abi}^*(z)$ and the temperature at the neck surface T_n^* . For simplicity, in this study the difference between the carotid arterial and average tissue temperatures is approximated as half of the maximum temperature difference in the cross-sectional plane (Weinbaum et al. 1997). Replacing $T_{abi}^*(z) - T_{t,avg}^*(z)$ by $0.5[T_{abi}^*(z) - T_n^*]$, one can rewrite Eq. (3) as

$$k_t \left\{ \left[\frac{1}{R^*} \frac{\partial}{\partial R^*} \left(R^* \frac{\partial T_t^*}{\partial R^*} \right) \right] + \frac{1}{R^{*2}} \frac{\partial^2 T_t^*}{\partial \phi^2} \right\} = -0.35 \omega \rho_{bl} C_{bl} [T_{abi}^*(z) - T_n^*], \quad (4)$$

$$R^* \leq R_t^*, \quad r_{ai}^* \geq a_{ai}^*, \quad r_{vi}^* \geq a_{vi}^*, \quad L^* \geq z^* \geq 0.$$

The corresponding boundary conditions are the continuity of the temperature and heat flux on the surface of each blood vessel and a prescribed temperature at the surface of the tissue cylinder.

$$T_{ai,vi}^* = T_t^*, \quad \text{for } r_{ai,vi}^* = a_{ai,vi}^*, \quad i = 1, 2, 3, 4; \quad (5)$$

$$\frac{\partial T_{ai,vi}^*}{\partial r_{ai,vi}^*} = \frac{\partial T_t^*}{\partial r_{ai,vi}^*}, \quad \text{for } r_{ai,vi}^* = a_{ai,vi}^*, \quad i = 1, 2, 3, 4; \quad (6)$$

$$T_t^* = T_n^*, \quad \text{for } R = R_t. \quad (7)$$

Note that the thermal conductivities of the tissue and blood are assumed to be the same in this analysis.

Nondimensional parameters are introduced as follows:

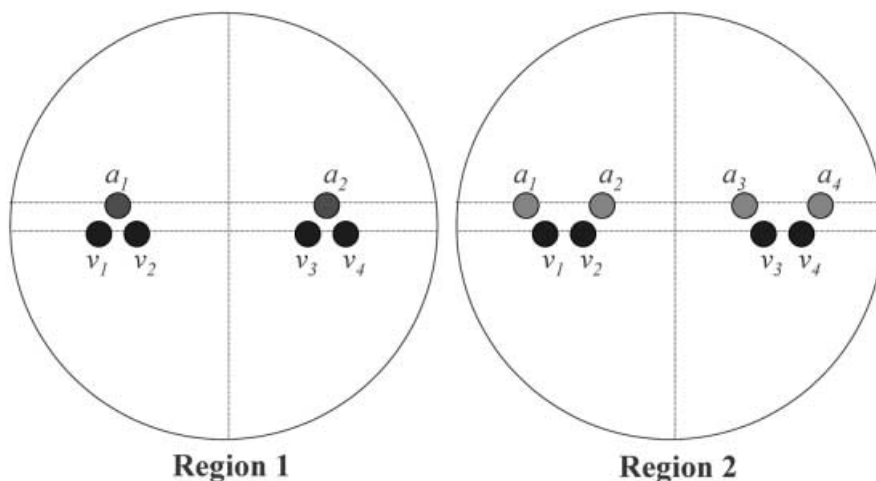


Fig. 3. The cross-sectional planes of regions 1 and 2

$$\begin{aligned}
r_a &= \frac{r_a^*}{a^*}, & r_v &= \frac{r_v^*}{a^*}, & s_a &= \frac{s_a^*}{a^*}, & s_v &= \frac{s_v^*}{a^*}, & R &= \frac{R^*}{a^*}, \\
R_t &= \frac{R_t^*}{a^*}, & z &= \frac{z^*}{a^*}, & L &= \frac{L^*}{a^*}, & l &= \frac{l^*}{a^*}, & Pe_a &= \frac{2\rho_{bl}C_{bl}a^*u_a^*}{k_{bl}}, \\
Pe_v &= \frac{2\rho_{bl}C_{bl}a^*u_v^*}{k_{bl}}, & T_a &= \frac{T_a^* - T_n^*}{T_{ab0}^* - T_n^*}, & T_v &= \frac{T_v^* - T_n^*}{T_{ab0}^* - T_n^*}, & T_t &= \frac{T_t^* - T_n^*}{T_{ab0}^* - T_n^*}.
\end{aligned} \tag{8}$$

All the length variables are scaled by the radius of the blood vessel a^* , which is the same for the arteries and veins. The temperatures are scaled by $T_{ab0}^* - T_n^*$, which is the maximum temperature variation within the tissue region. The temperature T_{ab0}^* is the artery bulk temperature at $z^* = 0$ in region 1 or at $z^* = L_1^*$ in region 2.

Based on the above assumptions and definitions, the dimensionless energy equations for the artery, vein, tissue, and the boundary conditions can be written

$$\begin{aligned}
\frac{1}{r_{ai}} \frac{\partial}{\partial r_{ai}} \left(r_{ai} \frac{\partial T_{ai}}{\partial r_{ai}} \right) + \frac{1}{r_{ai}^2} \frac{\partial^2 T_{ai}}{\partial \phi_{ai}^2} &= Pe_{ai} (1 - r_{ai}^2) \frac{dT_{abi}}{dz}, & r_{ai} &\leq 1, & i &= 1, 2, 3, 4; \\
\frac{1}{r_{vi}} \frac{\partial}{\partial r_{vi}} \left(r_{vi} \frac{\partial T_{vi}}{\partial r_{vi}} \right) + \frac{1}{r_{vi}^2} \frac{\partial^2 T_{vi}}{\partial \phi_{vi}^2} &= -Pe_{vi} (1 - r_{vi}^2) \frac{dT_{vbi}}{dz}, & r_{vi} &\leq 1, & i &= 1, 2, 3, 4;
\end{aligned} \tag{9}$$

$$\frac{1}{R} \frac{\partial}{\partial R} \left(R \frac{\partial T_t}{\partial R} \right) + \frac{1}{R^2} \frac{\partial^2 T_t}{\partial \phi^2} = -0.35 \frac{\omega \rho_{bl} C_{bl} a^{*2}}{k_t} T_{abi}, \quad R \leq R_t, \quad r_{ai} > 1, \quad r_{vi} > 1;$$

$$T_{ai,vi} = T_t, \quad \text{for } r_{ai,vi} = 1, \quad i = 1, 2, 3, 4; \tag{10}$$

$$\frac{\partial T_{ai,vi}}{\partial r_{ai,vi}} = \frac{\partial T_t}{\partial r_{ai,vi}}, \quad \text{for } r_{ai,vi} = 1, \quad i = 1, 2, 3, 4; \tag{11}$$

$$T_t = 0, \quad \text{for } R = R_t. \tag{12}$$

In Eq. (9) T_{abi} and T_{vbi} are the artery and vein bulk temperatures, respectively. These bulk temperatures are defined as

$$T_{abi}(z) = \frac{2}{\pi} \int_{-\pi}^{\pi} \int_0^1 T_{ai} (1 - r_{ai}^2) r_{ai} dr_{ai} d\phi_{ai}, \quad i = 1, 2, 3, 4; \tag{13}$$

$$T_{vbi}(z) = \frac{2}{\pi} \int_{-\pi}^{\pi} \int_0^1 T_{vi} (1 - r_{vi}^2) r_{vi} dr_{vi} d\phi_{vi}, \quad i = 1, 2, 3, 4.$$

3

Solution for the neck model

In this section, the solution for the boundary value problem outlined in Sect. 2 is presented. As shown in Fig. 3, the neck is divided into two regions of interest. Two and four arteries are located in region 1 and region 2, respectively, while there are four veins in each region. In each region, the governing equations, Eqs. (1) and (2), are written for blood vessels. The governing equation for the tissue is expressed by Eq. 4. The corresponding boundary conditions and matching conditions are given by Eq. (5).

3.1

Solution for region 1

Region 1 ($0 \leq z \leq L_1$) consists of a total of six blood vessels. The right and left common carotid arteries, which are located symmetrically on either side of the neck, will interact individually with the internal and external jugular vein on the right and left side, respectively. Using a similar approach to

that outlined in Wu et al. (1993) and Zhu (2000), the solution for the temperature of each blood vessel temperature in region 1 and the surrounding tissue can be decomposed into two parts, a homogeneous solution and a particular solution. The detailed derivation is given in the previous analyses (Wu et al. 1993; Zhu 2000). After solving the boundary value problem in the cross-sectional plane, the axial thermal interaction in the axial direction among the blood vessels in region 1 leads to the following equations:

$$\begin{aligned}
T_{ab1} &= \sum_{i=1}^2 B_{a1-ai} \frac{dT_{abi}}{dz} + \sum_{j=1}^4 B_{a1-vj} \frac{dT_{vbj}}{dz} + 0.35B_{a1} T_{ab1}, \\
T_{ab2} &= \sum_{i=1}^2 B_{a2-ai} \frac{dT_{abi}}{dz} + \sum_{j=1}^4 B_{a2-vj} \frac{dT_{vbj}}{dz} + 0.35B_{a2} T_{ab2}, \\
T_{vb1} &= \sum_{i=1}^2 B_{v1-ai} \frac{dT_{abi}}{dz} + \sum_{j=1}^4 B_{v1-vj} \frac{dT_{vbj}}{dz} + 0.35B_{v1} T_{ab1}, \\
T_{vb2} &= \sum_{i=1}^2 B_{v2-ai} \frac{dT_{abi}}{dz} + \sum_{j=1}^4 B_{v2-vj} \frac{dT_{vbj}}{dz} + 0.35B_{v2} T_{ab1}, \\
T_{vb3} &= \sum_{i=1}^2 B_{v3-ai} \frac{dT_{abi}}{dz} + \sum_{j=1}^4 B_{v3-vj} \frac{dT_{vbj}}{dz} + 0.35B_{v3} T_{ab2}, \\
T_{vb4} &= \sum_{i=1}^2 B_{v4-ai} \frac{dT_{abi}}{dz} + \sum_{j=1}^4 B_{v4-vj} \frac{dT_{vbj}}{dz} + 0.35B_{v4} T_{ab2}.
\end{aligned} \tag{14}$$

The coefficients in the coupled equations are functions of the blood-flow Peclet number and the geometric parameters, such as the vessel eccentricity and the vessel center-to-center spacing. The coefficients are listed in the following equation

$$\begin{aligned}
B_{ai-ai} &= -\frac{Pe_{ai}}{4} \left\{ \ln \left[R_t \left(1 - \frac{s_{ai}^2}{R_t^2} \right) \right] + \frac{11}{24} \right\}; \\
B_{ai-aj} &= -\frac{Pe_{aj}}{4} \left[\ln \left(\frac{R_t}{l_{ai-aj}} \sqrt{1 - \frac{2s_{ai}s_{aj}}{R_t^2} \cos \phi_{ai-aj} + \frac{s_{ai}^2 s_{aj}^2}{R_t^2}} \right) \right], \quad i \neq j; \\
B_{vj-vj} &= \frac{Pe_{vj}}{4} \left\{ \ln \left[R_t \left(1 - \frac{s_{vj}^2}{R_t^2} \right) \right] + \frac{11}{24} \right\}; \\
B_{vi-vj} &= \frac{Pe_{vj}}{4} \left[\ln \left(\frac{R_t}{l_{vi-vj}} \sqrt{1 - \frac{2s_{vi}s_{vj}}{R_t^2} \cos \phi_{vi-vj} + \frac{s_{vi}^2 s_{vj}^2}{R_t^2}} \right) \right], \quad i \neq j; \\
B_{ai-vj} &= \frac{Pe_{vj}}{4} \left[\ln \left(\frac{R_t}{l_{ai-vj}} \sqrt{1 - \frac{2s_{ai}s_{vj}}{R_t^2} \cos \phi_{ai-vj} + \frac{s_{ai}^2 s_{vj}^2}{R_t^2}} \right) \right], \quad B_{ai} = \frac{1\omega\rho_{bl}C_{bl}a^{*2}}{4k_t} (R_t^2 - s_{ai}^2 + 0.5); \\
B_{vj-ai} &= -\frac{Pe_{ai}}{4} \left[\ln \left(\frac{R_t}{l_{vj-ai}} \sqrt{1 - \frac{2s_{vj}s_{ai}}{R_t^2} \cos \phi_{vj-ai} + \frac{s_{vj}^2 s_{ai}^2}{R_t^2}} \right) \right], \quad B_{vj} = \frac{1\omega\rho_{bl}C_{bl}a^{*2}}{4k_t} (R_t^2 - s_{vj}^2 + 0.5).
\end{aligned} \tag{15}$$

Considering that $T_{ab1} = T_{ab2}$, $T_{vb1} = T_{vb4}$, and $T_{vb2} = T_{vb3}$ along their entire length because of symmetry, one may rewrite Eq. (14) as

$$\begin{aligned}
T_{ab1} &= (B_{a1-a1} + B_{a1-a2}) \frac{dT_{ab1}}{dz} + (B_{a1-v1} + B_{a1-v4}) \frac{dT_{vb1}}{dz} + (B_{a1-v2} + B_{a1-v3}) \frac{dT_{vb2}}{dz} + 0.35B_{a1}T_{ab1}, \\
T_{vb1} &= (B_{v1-a1} + B_{v1-a2}) \frac{dT_{ab1}}{dz} + (B_{v1-v1} + B_{v1-v4}) \frac{dT_{vb1}}{dz} + (B_{v1-v2} + B_{v1-v3}) \frac{dT_{vb2}}{dz} + 0.35B_{v1}T_{ab1}, \\
T_{vb2} &= (B_{v2-a1} + B_{v2-a2}) \frac{dT_{ab1}}{dz} + (B_{v2-v1} + B_{v2-v4}) \frac{dT_{vb1}}{dz} + (B_{v2-v2} + B_{v2-v3}) \frac{dT_{vb2}}{dz} + 0.35B_{v2}T_{ab1}.
\end{aligned} \tag{16}$$

The solution for Eq. (16) requires specification of three boundary conditions in the axial direction. For countercurrent flow, these boundary conditions are the prescribed bulk temperatures at the inlets of the vessels. The inlet temperature of the common carotid artery $T_{ab1}(0)$ is always equal to 1. The venous inlet temperatures $T_{vb1}(L_1)$ and $T_{vb2}(L_1)$ are unknown. The temperature continuity requires that the temperature of the jugular vein from region 1 to region 2 should be the same at the interface $z = L_1$. These boundary conditions are written as

$$\begin{aligned}
z = 0, \quad T_{ab1} &= 1; \\
z = L_1, \quad T_{vb1}|_{\text{region 1}} &= T_{vb1}|_{\text{region 2}}, \quad \text{and} \quad T_{vb2}|_{\text{region 1}} = T_{vb2}|_{\text{region 2}}.
\end{aligned} \tag{17}$$

3.2

Solution for region 2

Region 2 ($L_1 \leq z \leq L$) consists of eight blood vessels since the common carotid artery divides into the external and internal carotid arteries. The fundamental difference between region 2 and region 1 is that the vessel eccentricity of the carotid arteries and the vessel center-to-center spacing may vary in the axial direction, as shown in Fig. 1. Similarly, the axial thermal interaction is expressed by eight coupled ordinary differential equations, which are given by

$$\begin{aligned}
T_{ab1} &= \sum_{i=1}^4 B_{a1-ai} \frac{dT_{abi}}{dz} + \sum_{j=1}^4 B_{a1-vj} \frac{dT_{vbj}}{dz} + 0.35B_{a1}T_{ab1}, \\
T_{ab2} &= \sum_{i=1}^4 B_{a2-ai} \frac{dT_{abi}}{dz} + \sum_{j=1}^4 B_{a2-vj} \frac{dT_{vbj}}{dz} + 0.35B_{a2}T_{ab1}, \\
T_{ab3} &= \sum_{i=1}^4 B_{a3-ai} \frac{dT_{abi}}{dz} + \sum_{j=1}^4 B_{a3-vj} \frac{dT_{vbj}}{dz} + 0.35B_{a3}T_{ab3}, \\
T_{ab4} &= \sum_{i=1}^4 B_{a4-ai} \frac{dT_{abi}}{dz} + \sum_{j=1}^4 B_{a4-vj} \frac{dT_{vbj}}{dz} + 0.35B_{a4}T_{ab3}, \\
T_{vb1} &= \sum_{i=1}^4 B_{v1-ai} \frac{dT_{abi}}{dz} + \sum_{j=1}^4 B_{v1-vj} \frac{dT_{vbj}}{dz} + 0.35B_{v1}T_{ab1}, \\
T_{vb2} &= \sum_{i=1}^4 B_{v2-ai} \frac{dT_{abi}}{dz} + \sum_{j=1}^4 B_{v2-vj} \frac{dT_{vbj}}{dz} + 0.35B_{v2}T_{ab1}, \\
T_{vb3} &= \sum_{i=1}^4 B_{v3-ai} \frac{dT_{abi}}{dz} + \sum_{j=1}^4 B_{v3-vj} \frac{dT_{vbj}}{dz} + 0.35B_{v3}T_{ab3}, \\
T_{vb4} &= \sum_{i=1}^4 B_{v4-ai} \frac{dT_{abi}}{dz} + \sum_{j=1}^4 B_{v4-vj} \frac{dT_{vbj}}{dz} + 0.35B_{v4}T_{ab3}.
\end{aligned} \tag{18}$$

The coefficients in these coupled equations are given by Eq. (15). One notes that these coefficients may be functions of the axial distance z . Equation (18) can be further reduced to four coupled equations by taking the symmetry into account. Thus,

$$\begin{aligned}
T_{ab1} &= (B_{a1-a1} + B_{a1-a3}) \frac{dT_{ab1}}{dz} + (B_{a1-v1} + B_{a1-v3}) \frac{dT_{vb1}}{dz} + (B_{a1-a2} + B_{a1-a4}) \frac{dT_{ab2}}{dz} \\
&\quad + (B_{a1-v2} + B_{a1-v4}) \frac{dT_{vb2}}{dz} + 0.35B_{a1}T_{ab1}, \\
T_{ab2} &= (B_{a2-a1} + B_{a2-a3}) \frac{dT_{ab1}}{dz} + (B_{a2-v1} + B_{a2-v3}) \frac{dT_{vb1}}{dz} + (B_{a2-a2} + B_{a2-a4}) \frac{dT_{ab2}}{dz} \\
&\quad + (B_{a2-v2} + B_{a2-v6}) \frac{dT_{vb2}}{dz} + 0.35B_{a2}T_{ab1}, \\
T_{vb1} &= (B_{v1-a1} + B_{v1-a3}) \frac{dT_{ab1}}{dz} + (B_{v1-v1} + B_{v1-v3}) \frac{dT_{vb1}}{dz} + (B_{v1-a2} + B_{v1-a4}) \frac{dT_{ab2}}{dz} \\
&\quad + (B_{v1-v2} + B_{v1-v6}) \frac{dT_{vb2}}{dz} + 0.35B_{v1}T_{ab1}, \\
T_{vb2} &= (B_{v2-a1} + B_{v2-a3}) \frac{dT_{ab1}}{dz} + (B_{v2-v1} + B_{v2-v3}) \frac{dT_{vb1}}{dz} + (B_{v2-a2} + B_{v2-a4}) \frac{dT_{ab2}}{dz} \\
&\quad + (B_{v2-v2} + B_{v2-v6}) \frac{dT_{vb2}}{dz} + 0.35B_{v2}T_{ab1}. \tag{19}
\end{aligned}$$

The corresponding boundary conditions and matching conditions in the axial direction are

$$\begin{aligned}
z = L_1, \quad T_{ab1} \Big|_{\text{region 1}} &= T_{ab1} \Big|_{\text{region 2}} = T_{ab2} \Big|_{\text{region 2}}. \\
z = L, \quad T_{vb1} = T_{vb2} &= \text{prescribed value}. \tag{20}
\end{aligned}$$

The axial thermal interaction in region 2 is solved using a finite difference method and Gauss–Siedel iteration. Axial temperature gradients in Eqs. (16) and (19) are discretized using the central difference scheme. The accuracy of these approximations is second order in space. A uniform grid size (0.25 mm) is used in the axial direction. Once the nodal network has been established and the discretized equation has been written for each node, the problem is reduced to a system of linear algebraic equations for both regions 1 and 2. Gauss–Siedel iteration is then used to solve the linear algebraic equations until the results converge. Based on the algorithm, a FORTRAN code was written and run on a personal computer. The program was tested to ensure that the variations in the grid size or the number of iterations yielded less than 0.5% change in the final results.

4 Results

The thermal properties and the sizes of the vessels used in the neck model are listed in Table 1. In region 2, s^* does not remain constant because the common carotid artery bifurcates into the internal and external carotid arteries, which move toward and away, respectively, from the center of the neck cylinder. Therefore, vessel eccentricity in the neck model is a function of the axial coordinate z^* . The center-to-center spacing between any two blood vessels l^* , which depends on the eccentricity, also varies along the axial direction. As shown in Fig. 2, the veins are located along the x -axis in the cross-sectional plane, while the arteries are located with a small offset ($h^* = 5$ mm) from the x -axis. The length of each region in the neck model, L_1^* or L_2^* , is chosen to be 125 mm, which is half of the total axial length of the neck cylinder. In the neck model, it is assumed that of the total blood flow in each of the common carotid arteries (240 ml/min), 70% and 30% are in the internal and external carotid arteries, respectively. Similarly, the internal and external jugular veins collect 70% and 30% of the total blood, respectively (Nunneley and Nelson 1994).

Figure 4 shows the temperature distribution along the common, internal, and external carotid arteries during hyperthermia when $T_n^* = 20$ °C and $T_{vbl}^* = 20$ °C. The combined total blood temperature drop along the common and internal carotid arteries is approximately 0.87 °C, of which 0.34 °C occurs along the common carotid artery and 0.53 °C occurs along the internal carotid artery. Note that a larger temperature decrease (~ 1.3 °C) occurs along the common and external carotid arteries, since the external carotid artery runs obliquely toward the surface of the neck skin and it has a relatively small blood flow rate (72 ml/min).

The temperature distribution in the carotid arteries during neck surface cooling is illustrated in Fig. 5. The overall temperature decay along the common and internal carotid arteries before it reaches

Table 1. Thermal properties and vascular geometry in the neck model

Thermal properties	Geometry and blood flow	
	Region 1	Region 2
$\rho_{bl} = \rho_t = 1000 \text{ kg/m}^3$, $C_{bl} = 3600 \text{ J/kg K}$, $k_{bl} = k_t = 0.54 \text{ W/mK}$	$R_t^* = 60 \text{ mm}$	$R_t^* = 60 \text{ mm}$
	$a_a^* = a_v^* = 2.5 \text{ mm}$	$a_a^* = a_v^* = 2.5 \text{ mm}$
	$s_{v1}^* = s_{v4}^* = 36.2 \text{ mm}$	$s_{ai}^*(z)$ $s_{v1}^* = s_{v4}^* = 36.2 \text{ mm}$
	$s_{v2}^* = s_{v3}^* = 23.8 \text{ mm}$	$s_{v2}^* = s_{v3}^* = 23.8 \text{ mm}$
	$l_{a1-v1}^* = l_{a1-v2}^* = 6.2 \text{ mm}$	$l^*(z)$
	$L_1^* = 125 \text{ mm}$	$L_2^* = 125 \text{ mm}$
	$h^* = 5 \text{ mm}$	$h^* = 5 \text{ mm}$
	$Q_{a1} = Q_{a2} = 240 \text{ ml/min}$	$Q_{a1} = Q_{a4} = Q_{v1} = Q_{v4} = 72 \text{ ml/min}$
	$Q_{v1} = Q_{v4} = 72 \text{ ml/min}$	$Q_{a2} = Q_{a3} = Q_{v2} = Q_{v3} = 168 \text{ ml/min}$
	$Q_{v2} = Q_{v3} = 168 \text{ ml/min}$	$\omega = 0 \sim 3.3 \times 10^{-4} \text{ s}^{-1}$
	$\omega = 0 \sim 3.3 \times 10^{-4} \text{ s}^{-1}$	-

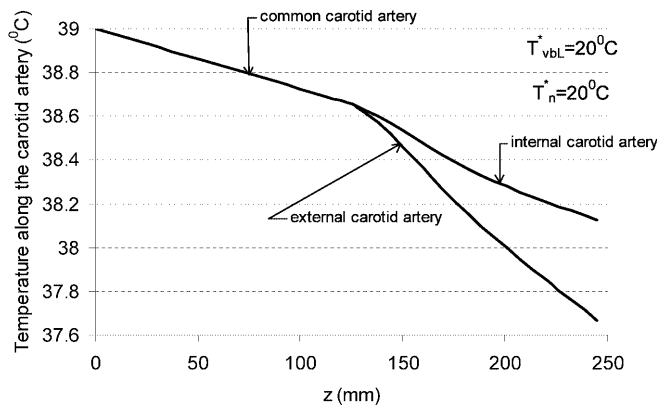


Fig. 4. Temperature distribution along the common, internal and external carotid arteries during hyperthermic conditions

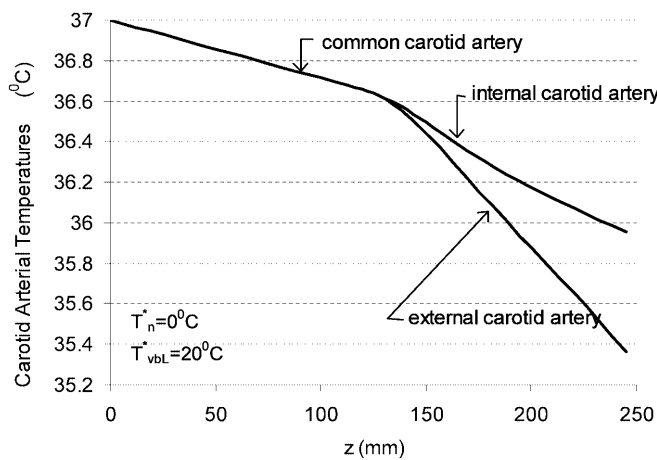


Fig. 5. Temperature distribution along the common, internal and external carotid arteries during hypothermic conditions

the base of the brain is approximately $1.1 \text{ }^\circ\text{C}$ when $T_{vbl}^* = 20 \text{ }^\circ\text{C}$ and $T_n^* = 0 \text{ }^\circ\text{C}$. Note that the temperature drop along the common and internal carotid arteries increases approximately 32% during hypothermia in comparison with that during hyperthermic conditions.

Figure 6 examines the contributions of both conductive heat loss and countercurrent heat exchange to the axial temperature distribution in the carotid arteries. As shown in Fig. 6, during hypothermia ($T_n^* = 0 \text{ }^\circ\text{C}$), the temperature in the common and internal carotid arteries drops more than 43% when

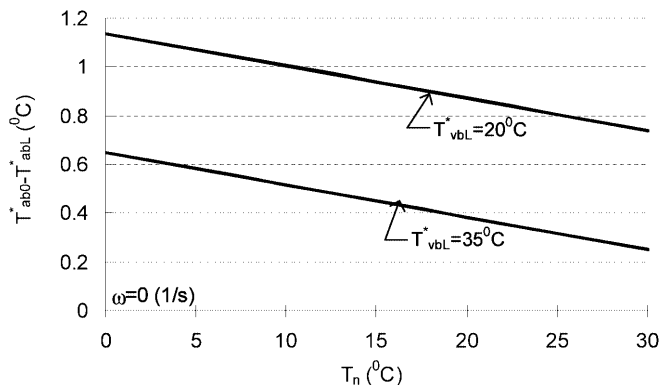


Fig. 6. Effect of neck surface temperature on the temperature decrease along the common and internal carotid arteries for different venous inlet temperatures

$T_{vbL}^* = 20\text{ }^\circ\text{C}$ increases from 20 to 35 $^\circ\text{C}$. The temperature $T_{vbL}^* = 35\text{ }^\circ\text{C}$ can be viewed as the limiting condition for which the countercurrent heat exchange is negligible. It is suggested that countercurrent heat exchange could account for approximately 43% of the arterial cooling during hypothermia. A similar temperature drop induced by the countercurrent heat exchange can be found when $T_n^* = 20\text{ }^\circ\text{C}$, except that the relative contribution of the countercurrent heat exchange is more evident (66%).

The influence of the local blood perfusion in the neck tissue on the arterial cooling is illustrated in Fig. 7 for hyperthermic conditions. It is shown that a change in the local blood perfusion rate from 0 to 0.00033 1/s produces an approximately 20% decrease in the arterial cooling along the common and internal carotid arteries. This is expected since local blood perfusion acts as a heat source in the temperature field of the neck tissue and may change the radial temperature distribution significantly.

5 Discussion and conclusions

The results of the neck model have shown that the overall temperature decay along the common and internal carotid arteries before it reaches the base of the brain is approximately 0.87 $^\circ\text{C}$ under hyperthermic conditions and 1.1 $^\circ\text{C}$ under hypothermic conditions. Various factors, including the local blood perfusion rate, blood vessel bifurcation in the neck, and blood vessel pairs on both sides of the neck that were not considered in an earlier theoretical model (Zhu 2000), are taken into consideration in this model. Note that the temperature decay along the common and internal carotid arteries is the same as the temperature difference between the body core and arterial blood at the base of the brain. Thus this model provides a reasonable estimate of the temperature difference between the body core and the arterial blood supplied to the brain.

The simulated result suggests that the main factor affecting the cooling capacity of the arterial blood is the blood flow rate in the carotid arteries and jugular veins. Unlike smaller blood vessels, in which the thermal equilibration length is much shorter than their physical length, the limited cooling capacity along the carotid arteries is primarily due to the high flow velocity in these blood vessels in the human neck. A previous theoretical study (Weinbaum et al. 1984) demonstrated that the thermal equilibration length is approximately proportional to $1/Q$, where Q is the flow rate in the blood vessel. In this study the blood flow rate is assumed equal to 240 ml/min in the common carotid arteries. Thus, one can extrapolate the current calculation to other situations with different blood flow rates. It is

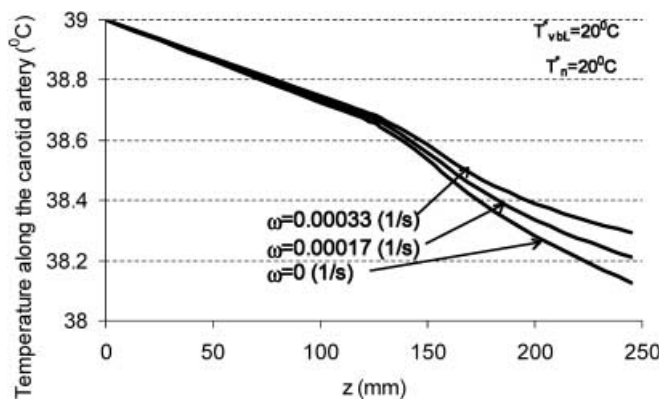


Fig. 7. Temperature distribution along the common and internal carotid arteries as a function of the local blood perfusion rate in the neck muscle during hyperthermic condition

expected that doubling the blood flow rate in the common carotid arteries (480 ml/min) would lead to a 50% decrease in the temperature decay along the carotid arteries. On the other hand, the temperature drop along the carotid arteries would be twice that in the current simulated condition if the blood flow rate in the carotid arteries is decreased by 50% (120 ml/min).

In this study the effect of local blood perfusion in the skeletal muscle of the neck has been tested. The local blood perfusion rate, if it is not very large, plays a minor role in the arterial cooling. During hypothermia when the neck and head surface are packed with ice, local thermoregulation may result in vasoconstriction in the neck muscle, and thus a small blood perfusion rate in the tissue is reasonable. During heavy exercise, blood flow may be redistributed from nonexercise organs or muscle to exercise muscle to maintain the increased nutrient need there. It is still not quite clear how the elevated body core temperature during hyperthermia affects the local blood perfusion rate in the neck muscle. It is possible that physiological reactions to hyperthermia are probably controlled by the central nervous system (CNS). It has been suggested that the CNS could integrate the signals from thermally sensitive sites distributed within the body and the skin, which may include the core body temperature and the temperature of the skin.

Other factors, such as the vessel bifurcation, thermal interaction between blood vessel pairs on both sides of the neck, and the accuracy of the modified Pennes perfusion term, seem to have very limited effects on the arterial cooling along the carotid arteries. If one compares the current simulated results with the predictions of the previous model (Zhu 2000) in which a pair of countercurrent blood vessels is embedded in a neck tissue cylinder, the temperature drops along the common and internal carotid arteries are very similar, provided that the same blood flow rate is used. This implies that taking into consideration the vessel bifurcation and blood vessel pair thermal interaction should not change the result significantly. In the modified Pennes perfusion term, an average value of 0.7 is used to account for the venous rewarming in the skeletal muscle. In addition, the temperature difference on the right side of Eq. (3) is assumed to be equal to half of the maximum temperature difference in the cross-sectional plane. This value was estimated from a previous analysis of thermal equilibration along a single pair of countercurrent vessels embedded in a tissue cylinder (Weinbaum et al. 1997). It may not be very accurate for the current vascular geometry. Based on an approach developed by Zhu et al. (1996), the current model can certainly be modified to determine the relationship among the average tissue temperature, the arterial temperature, and the temperature at the tissue cylinder surface. However, as shown in Eqs. (3) or (4), any variation from this chosen value will only result in a change in the strength of the modified perfusion source term. Notice that in Fig. 7 doubling the strength of the perfusion term (ω varies from 0.00017 to 0.00033 s^{-1}) leads to less than 10% variation in the result. Thus, the error caused by the uncertainty of this value should be small unless the local blood perfusion rate is very large. Similarly, the deviation from the chosen value 0.7 for the venous rewarming could also have a minor effect on the thermal equilibration along the carotid arteries.

Two driving forces determine the arterial cooling capacity. Cooling along the arteries depends on the inlet temperature difference between the carotid artery and jugular vein. The chief veins draining the head and neck are the internal jugular veins, which collect blood from the brain tissue and neck. The external jugular veins drain blood from the parotid glands, facial muscles, scalp, and other superficial structures. The venous return temperature should be determined by the mixture of the warm blood from the brain tissue and the cold blood from the superficial parts such as the nasal areas and the scalp. Therefore, to get an accurate estimate of the venous return temperature, a model that accounts for the thermal variation in both the neck and brain must be developed. We consider the experimentally measured canthus temperature of 18 °C (Deklunder et al. 1991) as the lower limit for the venous return temperature. Obviously, the contribution of countercurrent heat exchange to the arterial cooling could be significantly decreased if the venous return temperature in both the internal and external jugular veins is much higher than 20 °C, as indicated by the simulated results.

Another driving force for arterial cooling is the neck surface temperature. During hypothermia, the lower limit of the neck temperature is 0 °C, which can be achieved if there is a good thermal contact between the interior surface of the cooling helmet and the neck surface. During hyperthermia, the temperature of the neck surface depends on various conditions, including air temperature, wind speed, local humidity, sweating on the skin surface, and heat transfer efficiency in the upper airway. Previous temperature measurement of the neck or scalp surface has shown that it varies from 23 °C to 35 °C during heavy exercise and/or under hot environmental conditions. It is believed that the low skin temperature is achieved by intensive sweating and low humidity in the surrounding environment.

In conclusion, in this study a theoretical model has been developed to evaluate the thermal equilibration along a branching carotid artery. Results of the present study could help one understand

the mechanism of selective brain cooling (SBC) in humans during hyperthermia. It can also be used to evaluate the feasibility of lowering the brain temperature effectively by placing ice pads on the neck surface or by wearing a cooling helmet. Our simulations suggest that the temperature of the body core is not a good indication of the temperature of the brain during either hyperthermic or hypothermic conditions.

References

- Baker, M.A.:** Brain cooling in endotherms in heat and exercise. *Ann Rev Physiol* 44 (1982) 85–96
- Barone, F.C.; Feuerstein, G.Z.; White, R.F.:** Brain cooling during transient focal ischemia provides complete neuroprotection. *Neurosci Biobehav Rev* 21 (1997) 31–44
- Cabanac, M.:** Selective brain cooling in humans: “fancy” and “fact”? *FASEB J* 7 (1993) 1143–1147
- Chato, J.C.:** Selected thermophysical properties of biological materials. In: Shitzer A, Eberhart RC (eds) *Heat transfer in biology and medicine*. Plenum, New York, (1985) pp 413–418
- Clark, R.S.B.; Kochanek, P.M.; Schiding, J.K.; White, M.; Palmer, A.M.; Dekosky, S.T.:** Mild posttraumatic hypothermia reduces mortality after severe controlled cortical impact in rats. *J Cerebral Blood Flow Metabol* 16 (1996) 253–261
- Ku, Y.E.; Montgomery, L.D.; Webbon, B.:** Hemodynamic and thermal responses to head and neck cooling in men and women. *Am J Phys Med Rehabil* 75 (1996) 443–450
- Marion, D.W.:** Treatment of traumatic brain injury with moderate hypothermia. *N Engl J Med* 336 (1997) 540–556
- Nielsen, B.:** Natural cooling of the brain during outdoor bicycling? *Pflugers Arch Ges Physiol Menschen Tiere* 411 (1988) 456–461
- Nunneley, S.A.; Nelson, D.A.:** Limitations on arterio-venous cooling of the blood supply to the human brain. *Eur J Appl Physiol* 69 (1994) 474–479
- Sirimanne, E.S.; Blumberg, R.M.; Bossana, D.; Gunning, M.; Edwards, A.D.; Gluckman, P.D.; Williams, C.E.:** The effect of prolonged modification of cerebral temperature on outcome after hypoxic-ischemic brain injury in the infant rat. *Pediatr Res* 39 (1996) 591–597
- Wass, C.T.; Lanier, W.L.; Hofer, R.E.; Scheithauer, B.W.; Andrews, A.G.:** Temperature changes of ≥ 1 °C alter functional neurological outcome and hispathology in a canine model of complete cerebral ischemia. *Anesthesiology* 83 (1995) 325–335
- Weinbaum, S.; Jiji, L.M.; Lemons, D.E.:** Theory and experiment for the effect of vascular microstructure on surface tissue heat transfer. 1. Anatomical foundation and model conceptualization. *ASME J Biomech Eng* 106 (1984) 321–330
- Weinbaum, S.; Xu, L.X.; Zhu, L.; Epkene, A.:** A new fundamental bioheat equation for muscle tissue. 1. Blood perfusion term. *ASME J Biomech Eng* 119 (1997) 278–288
- Wenger, C.B.:** More comments on “keeping a cool head”. *News Physiol Sci* 2 (1987) 150–151
- Wu, Y.; Weinbaum, S.; Jiji, L.M.:** A new analytic technique for 3-D heat transfer from a cylinder with two or more axially interacting eccentrically embedded vessels with application to countercurrent blood flow. *Int J Heat Mass Transfer* 36 (1993) 1073–1083
- Zhu, L.; Lemons, D.E.; Weinbaum, S.:** Microvascular thermal equilibration in rat cremaster muscle. *Ann Biomed Eng* 24 (1996) 109–123
- Zhu, L.:** Theoretical evaluation of contributions of heat conduction and countercurrent heat exchange in selective brain cooling in humans. *Ann Biomed Eng* 28 (2000) 269–277
- Zhu, L.; Diao, C.:** Theoretical simulation of temperature distribution in the brain during mild hypothermia treatment for brain injury. *Med Biol Eng Comput* 39 (2001) 681–687
- Zhu, M.; Weinbaum, S.; Jiji, L.M.:** Heat exchange between unequal countercurrent vessels asymmetrically embedded in a cylinder with surface convection. *Int J Heat Mass Transfer* 33 (1990) 2275–2284